

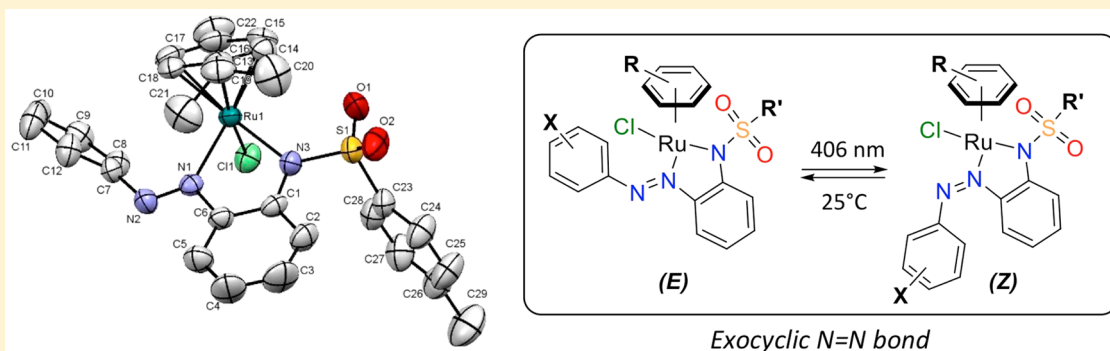
# Photoswitchable Arene Ruthenium Complexes Containing *o*-Sulfonamide Azobenzene Ligands

Claire Deo,<sup>†</sup> Nicolas Bogliotti,<sup>\*,†</sup> Rémi Métivier,<sup>†</sup> Pascal Retailleau,<sup>‡</sup> and Juan Xie<sup>\*,†</sup>

<sup>†</sup>PPSM, ENS Cachan, CNRS, Université Paris-Saclay, 94235 Cachan, France

<sup>‡</sup>Institut de Chimie des Substances Naturelles, CNRS UPR 2301, Université Paris-Sud, Université Paris-Saclay, 1, av. de la Terrasse, 91198 Gif-sur-Yvette, France

## S Supporting Information



**ABSTRACT:** A series of arene ruthenium complexes containing *o*-sulfonamide azobenzene ligands were synthesized and found to exhibit uncommon coordination pattern with an exocyclic N=N bond. Upon irradiation, these complexes cleanly undergo *E* → *Z* photoisomerization followed by thermal *Z* → *E* isomerization (upon resting in the dark) whose rate is dependent on the solvent, the nature of the arene group, the sulfonamide moiety, and azobenzene substitution, as revealed by structure–property studies.

## INTRODUCTION

The photoisomerization properties of azobenzene have been extensively exploited for the control of events at various scales and interfacing many fields such as molecular biology, pharmacology, chemistry, material sciences, physics, information, and data storage technology.<sup>1–10</sup> Azobenzene and its derivatives such as 2-(arylo)pyridines, 2-(arylo)pyrimidines, and 2-(arylo)imidazoles are also appealing compounds in coordination chemistry due to their interesting redox behavior and the strong M–L bonding resulting from their potent  $\pi$ -acceptor character.<sup>11</sup> Remarkably, these ligands have been frequently combined with ruthenium, and the resulting complexes have found promising applications in catalysis<sup>12–16</sup> and as cytotoxic agents toward various cancer cell lines.<sup>17–20</sup> These compounds most commonly exhibit bidentate or tridentate coordination patterns such as **I**,<sup>17–30</sup> **II**,<sup>13,16,31,32</sup> **III**,<sup>14,15,24,25,32,33</sup> and **IV**<sup>12</sup> (Figure 1). In each case, the N=N bond is located inside a chelate ring formed with the metal, thus preventing azobenzene photoisomerization. Only a few exceptions involving multimetallic species have been shown to maintain photoisomerization ability of azobenzene upon direct coordination of both nitrogen atoms of the N=N bond to the Ru atom.<sup>34–36</sup> More recent examples concern the photoisomerization of azobenzene-coupled metal complexes without coordination of the azobenzene moiety.<sup>37,38</sup>

We reasoned that structural modification of the ligand could affect the coordination pattern in such a way that the photoswitching ability of azobenzene would be maintained upon coordination to the metal center. The resulting organometallic complexes could be interesting candidates for the photocontrol of catalytic activity<sup>39–44</sup> and biological applications.<sup>1,3,5,9,45–47</sup> Here, we wish to report a new type of photoswitchable arene ruthenium complex containing *o*-sulfonamide azobenzenes as ligands (**V**; Figure 1) and describe their photoisomerization properties.

## RESULTS AND DISCUSSION

### Synthesis and Photophysics of Ligand 3 and Complex

**4.** The prototype *o*-tosylamide azobenzene **3**<sup>48</sup> was synthesized as described in Scheme 1 in order to investigate its behavior as a ligand for ruthenium. Commercially available *o*-phenylenediamine was tosylated under standard conditions (TsCl, pyridine) to yield **1**,<sup>49</sup> which underwent reaction with oxone to afford *o*-tosylaminonitrosobenzene (**2**) in 94% yield. This compound was treated under Mills conditions,<sup>8</sup> in the presence of aniline and acetic acid in refluxing toluene, to give the desired *o*-tosylaminoazobenzene ligand **3**. Finally, reaction

**Received:** October 15, 2015

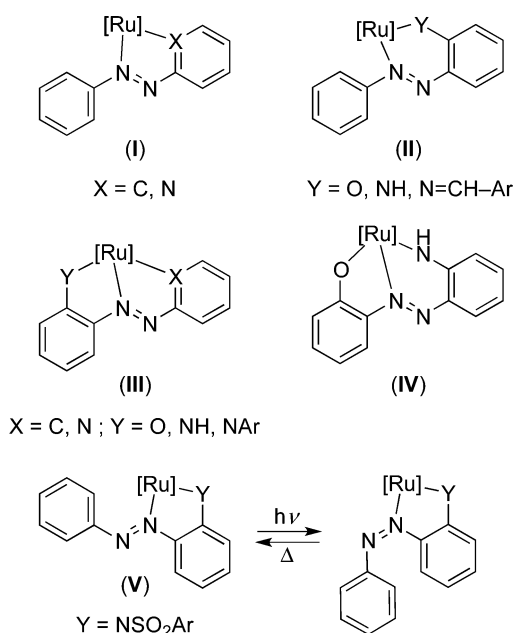
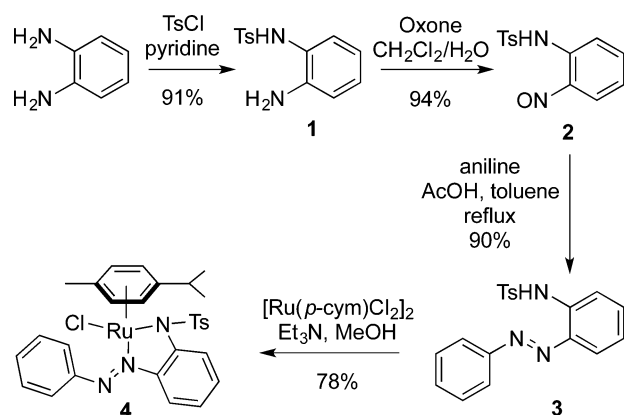


**Figure 1.** Common coordination pattern for ruthenium azobenzene complexes (I–IV) and a novel type of photoswitchable organometallic complex (V).

#### Scheme 1. Synthesis of Ligand 3 and Complex 4



with the ruthenium dimer  $[Ru(p\text{-cym})Cl_2]_2$  and triethylamine in methanol led to ruthenium complex **4** as a dark brown solid (78% yield). The structure of this complex was confirmed by  $^1H$  and  $^{13}C$  NMR spectroscopy, HRMS, and elemental analysis. Crystals suitable for X-ray crystallographic analysis were obtained by slow evaporation of a solution of the complex in  $CH_2Cl_2$ . The structure of complex **4** reveals a classical “three-legged piano-stool” configuration at the ruthenium atom, and most importantly, **3** acts as a bidentate N,N ligand forming a five-membered ring with an exocyclic  $N=N$  bond (Figure 2 and discussion below).

Preliminary spectroscopic and photophysical studies of ligand **3** and complex **4** were performed in MeCN. Free ligand **3** exhibits a strong absorption band at 324 nm ( $\epsilon = 16650 \pm 350 \text{ L mol}^{-1} \text{ cm}^{-1}$ ) assigned to a  $\pi \rightarrow \pi^*$  transition and a weak band at 454 nm ( $\epsilon = 800 \pm 10 \text{ L mol}^{-1} \text{ cm}^{-1}$ ) corresponding to a forbidden  $n \rightarrow \pi^*$  transition (black line, Figure 3). Complex **4** shows two bands of similar intensity at 319 nm ( $\epsilon = 9550 \pm 20 \text{ L mol}^{-1} \text{ cm}^{-1}$ ) and 421 nm ( $\epsilon = 6850 \pm 30 \text{ L mol}^{-1} \text{ cm}^{-1}$ ), both assigned mainly to intraligand  $\pi \rightarrow \pi^*$  transitions, and a

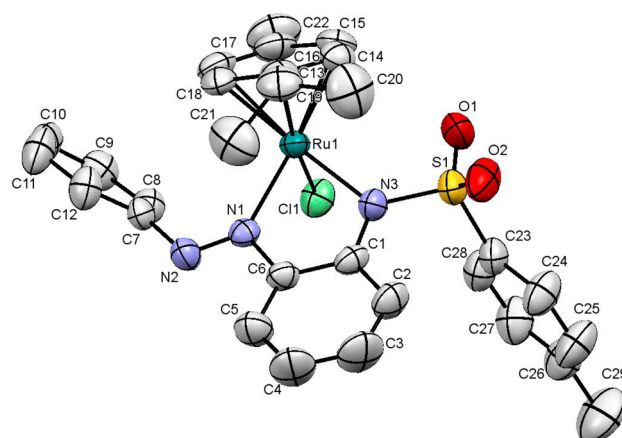


**Figure 2.** ORTEP representation (thermal ellipsoids drawn at 50% probability level) of complex **4** with the atom-numbering scheme. The hydrogen atoms have been omitted for clarity. Selected bond lengths (Å) and angles (deg): Ru–N1 = 2.081(2), Ru–N3 = 2.101(2), Ru–Cl1 = 2.3993(8), Ru–cent = 1.703(3), N1–N2 = 1.258(3), N3–S1 = 1.618(2); N3–Ru–Cl1 = 85.65(7), N3–Ru–N1 = 77.57(9), N1–Ru–Cl1 = 86.46(6).

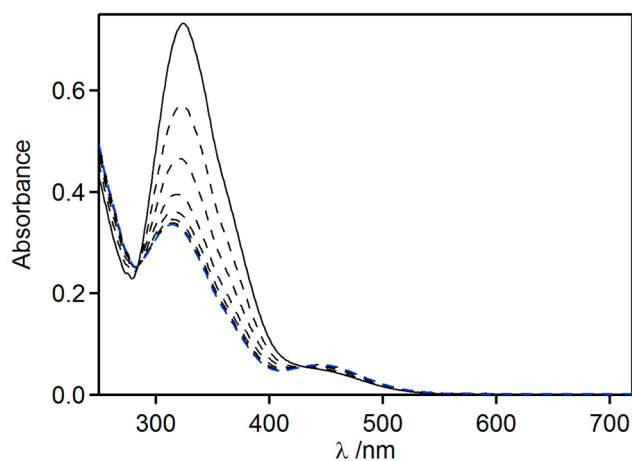


**Figure 3.** Absorption spectrum of ligand (*E*)-**3** in MeCN ( $C = 45 \mu\text{M}$ ) at 25 °C (black solid line) and its stepwise evolution upon 5 s irradiation pulses at 315 nm with  $P = 40 \text{ mW cm}^{-2}$  (black dashed lines). The blue dashed line corresponds to PSS.

weaker band in the visible region at 566 nm ( $\epsilon = 2750 \pm 20 \text{ L mol}^{-1} \text{ cm}^{-1}$ ) assigned mainly to Ru ( $4d^6$ )  $\rightarrow \pi^*$  transition (black line, Figure 4).<sup>20</sup>

As expected, irradiation at 315 nm of a solution of **3** in MeCN resulted in a steady decrease of the band at 324 nm, with two isosbestic points at 285 and 422 nm, revealing  $E \rightarrow Z$  photoisomerization of azobenzene moiety (Figure 3 and Scheme 2). Under these conditions, the photostationary state (PSS) was reached after ca. 35 s. Its composition was determined to be  $E:Z = 29:71$  by a combination of  $^1H$  NMR and UV–vis spectroscopy (see the Supporting Information for details). The half-life of (*Z*)-**3** (determined upon resting the sample in the dark at 25 °C) could not be precisely measured due to reproducibility issues, but several independent experiments indicated  $t_{1/2}(Z)$  values ranging from 1 to 4 h in MeCN. Similar behavior has already been reported for other azobenzene derivatives such as azopyridines and was attributed to their high sensitivity to traces of water or acid.<sup>50</sup> Attempts to buffer a solution of **3** in MeCN by addition of either 1% (v/v)

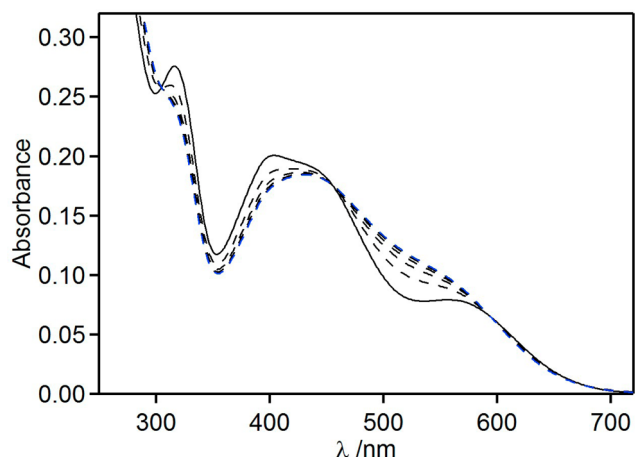
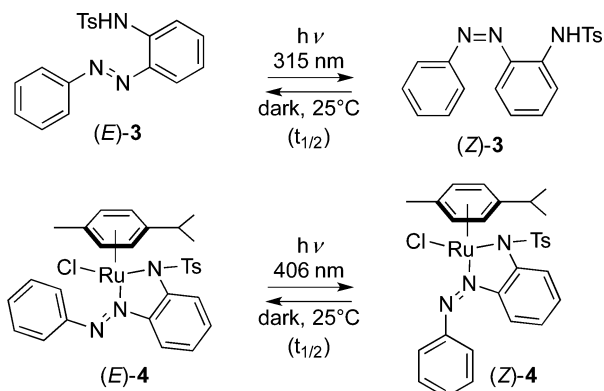


**Figure 4.** Absorption spectrum of ruthenium complex (*E*)-4 in MeCN ( $C = 30 \mu\text{M}$ ) at  $25^\circ\text{C}$  (black solid line) and its stepwise evolution upon 5 s irradiation pulses at 406 nm with  $P = 9 \text{ mW cm}^{-2}$  (black dashed lines). The blue dashed line corresponds to PSS.

#### Scheme 2. Photoswitching of Ligand 3 and Complex 4



$\text{H}_2\text{O}$  at pH 7 or 1% (v/v) TFA greatly shortened the half-lives of the *Z* isomer without improving reproducibility ( $t_{1/2}$  around 240 and 30 s, respectively).

Gratifyingly, complex 4 also undergoes photoisomerization upon irradiation at 406 nm in MeCN, as revealed by a concomitant steady decrease of the absorption band around 400 nm and increase around 515 nm, and the presence of an isosbestic point at 456 nm (Figure 4 and Scheme 2). The PSS was rapidly reached (in ca. 35 s), and the ratio *E*:*Z* = 56:44 was determined by the same method as for ligand 3 (see the Supporting Information). The rate of thermal back *Z* → *E* isomerization was determined to be much faster than that in the case of 3, with a reproducible  $t_{1/2}$  value of  $6.5 \pm 0.3 \text{ min}$  at  $25^\circ\text{C}$  in MeCN. It is noteworthy that such a switching process could be repeated over 10 times without any noticeable degradation of the complex (Figure 5).

**Photoisomerization Study of 4 by  $^1\text{H}$  NMR Spectroscopy.** Portions of the  $^1\text{H}$  NMR spectra of 4 in  $\text{CD}_3\text{CN}$  before and after irradiation are reported in Figure 6. The aromatic protons of the *p*-cymene moiety appear as four distinct signals: two doublets at 5.43 and 5.05 ppm corresponding to H14 and H15 and two broad signals at 6.21 and 3.51 ppm corresponding to H18 and H17, respectively (Figure 6). This significant perturbation of chemical shifts can be explained by the influence of the aryl group of azobenzene directly facing the *p*-cymene moiety (Figure 2), resulting in a strong shielding of

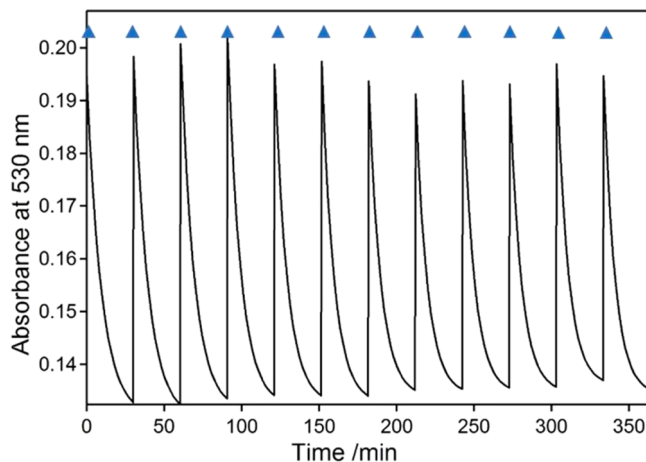


**Figure 5.** Fatigue resistance of complex 4 in MeCN ( $C = 60 \mu\text{M}$ ) upon alternating irradiation and resting (dark,  $25^\circ\text{C}$ ). Blue triangles refer to irradiation pulses at 406 nm.

H17 (ca. 1.5 ppm) located above the aromatic ring and deshielding of H18 (ca. 1 ppm) located on the side of the ring (Figure 6). Irradiation of (*E*)-4 at 406 nm resulted in the apparition of a new set of signals corresponding to (*Z*)-4. As a consequence of isomerization of the  $\text{N}=\text{N}$  bond, the aryl group of azobenzene does not exert any ring current effect; the *p*-cymene group in (*Z*)-4 thus appears as four well-defined doublets between 5.42 and 5.99 ppm (green arrows).

**Structure–Property Relationship in Arene Ruthenium *o*-Sulfonamide Azobenzenes.** Encouraged by these results, we decided to prepare other complexes, in order to investigate the influence of structure on photophysical properties. We focused on (i) changing the nature of sulfonamide group, (ii) introducing fluorine atoms on the benzene group, as such a modification is known to result in very long lived *Z* isomers,<sup>51,52</sup> and (iii) modifying the arene ligand on ruthenium (Figure 7).

The synthesis of complexes 7 and 9 is described in Scheme 3. Nitrosobenzene was treated with *o*-phenylenediamine under classical Mills conditions in the presence of acetic acid in refluxing toluene, to afford the amino azobenzene 5 in 46% yield.<sup>53</sup> Treatment with  $\text{MsCl}$  and pyridine in dichloromethane gave ligand 6, which was easily converted to complex 7 in 63% yield upon reaction with  $[\text{Ru}(p\text{-cym})\text{Cl}_2]_2$  and triethylamine in methanol. Reaction of 5 with triflic anhydride in  $\text{CH}_2\text{Cl}_2$  yielded 94% of ligand 8, which was converted to complex 9 in the presence of  $[\text{Ru}(p\text{-cym})\text{Cl}_2]_2$  in MeOH.

Initial attempts to react commercially available 2,6-difluoroaniline with the nitroso derivative 2 did not lead to the expected fluorinated ligand 11 (Scheme 4). However, when 2,6-difluoroaniline was transformed into the corresponding nitroso compound 10, followed by reaction with amine 1, ligand 11 was obtained in 24% yield. Then, formation of difluorinated complex 12 proceeded smoothly, as described for 4 and 7.

Modification of the aryl group has been shown previously to significantly affect the properties and reactivity of ruthenium arene complexes.<sup>54,55,20,56–59</sup> However, to the best of our knowledge, its influence on the isomerization properties of azobenzene ligands has never been investigated. Thus, we synthesized complexes 13 and 14, analogous to 4, in which the *p*-cymene ligand is replaced by benzene and hexamethylbenzene, respectively (Scheme 5). Standard reaction conditions,

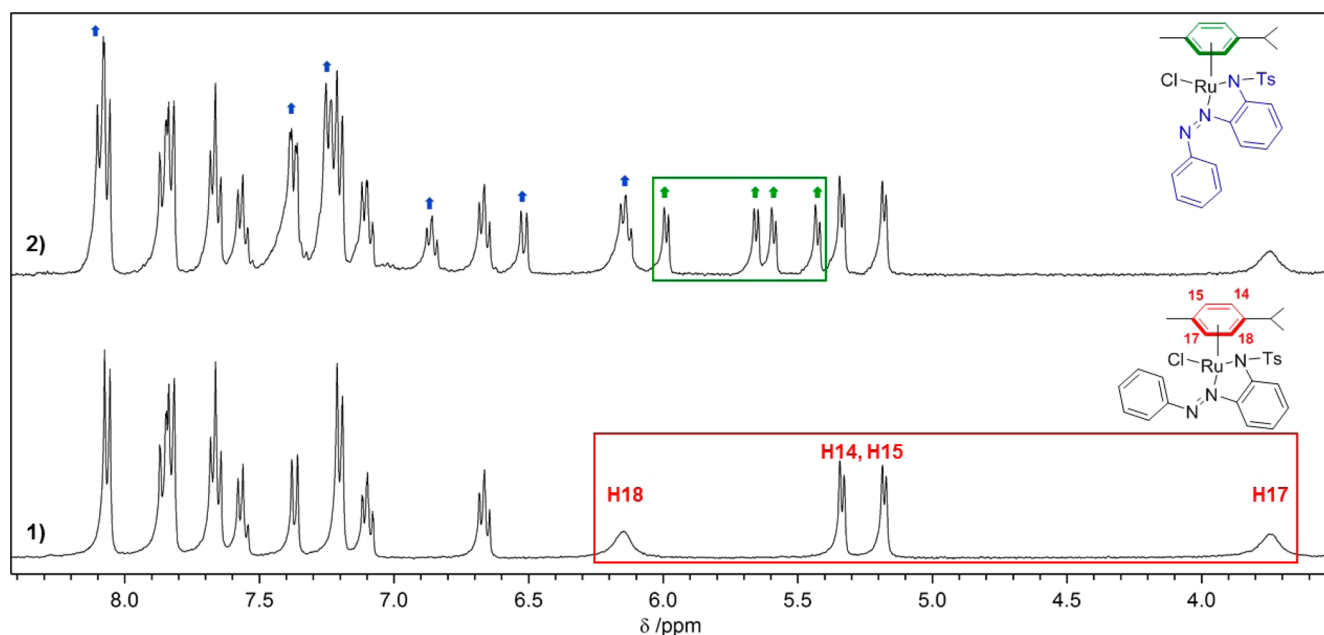


**Figure 6.** Portions of  $^1\text{H}$  NMR spectra of complex **4** in  $\text{CD}_3\text{CN}$  ( $C = 13 \text{ mM}$ ) (1) before irradiation and (2) after irradiation at 406 nm ( $P = 40 \text{ mW cm}^{-2}$ ,  $t = 15 \text{ min}$ ). The red and green frames indicate the signals corresponding to the aromatic protons of the *p*-cymene moiety of *E* and *Z* isomers, respectively; arrows indicate the signals corresponding to the *Z* isomer appearing upon irradiation.

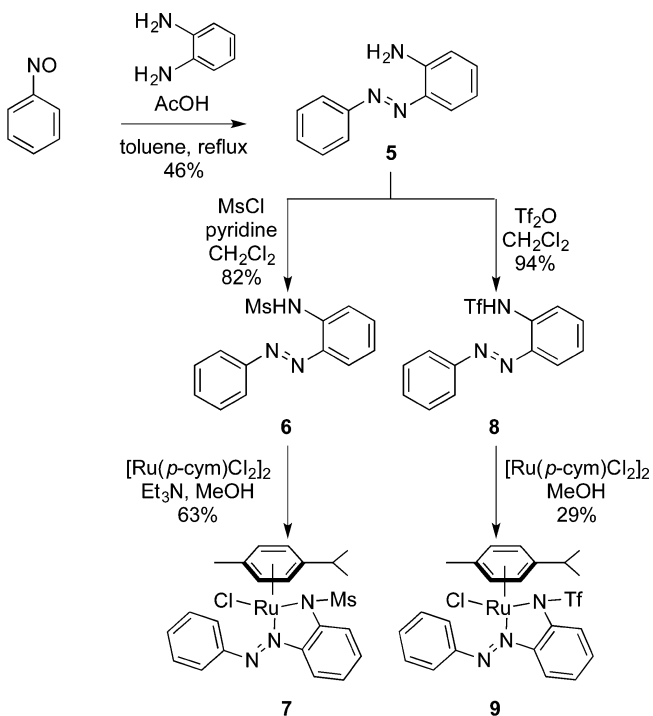
	Arene	R	X
<b>4:</b>	<i>p</i> -cym		H
<b>7:</b>	<i>p</i> -cym	—Me	H
<b>9:</b>	<i>p</i> -cym	—CF <sub>3</sub>	H
<b>12:</b>	<i>p</i> -cym		F
<b>13:</b>	bz		H
<b>14:</b>	hmbz		H

**Figure 7.** Ruthenium arene complexes investigated for structure–property relationships.

using  $[\text{Ru}(\text{C}_6\text{H}_6)\text{Cl}_2]_2$  or  $[\text{Ru}(\text{C}_6\text{Me}_6)\text{Cl}_2]_2$  and ligand **3** in the presence of  $\text{Et}_3\text{N}$  in MeOH, cleanly afforded the desired complexes in 83% and 75% yields as dark brown solids.

The molecular structures of the ruthenium complexes **4**, **7**, **9**, and **14** were determined by single crystal X-ray diffraction. Their representations along with atom numbering scheme are shown in Figure 2 and Figure 8, and selected bond lengths and

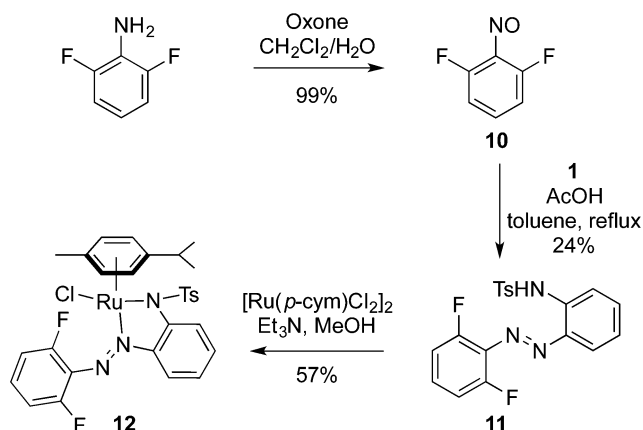
**Scheme 3.** Synthesis of Ligands **6** and **8** and Their Corresponding Complexes **7** and **9**



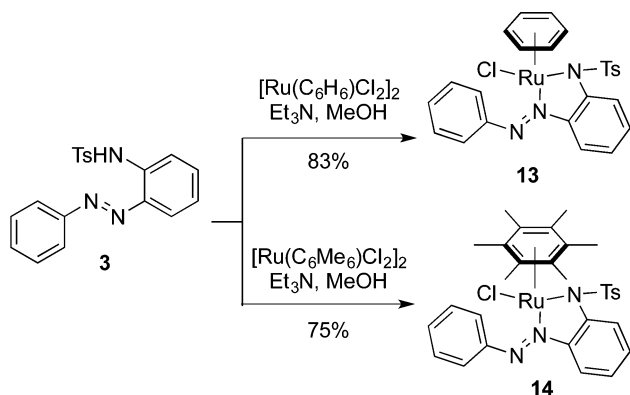
angles are given in Table 1. Complexes **4**, **7**, **9**, and **14** share similar structures, with ruthenium center in a pseudo-octahedral geometry in which the  $\eta^6$ -arene ligand occupies a face. The ruthenium–arene centroid distances (in the range between 1.702 and 1.714 Å) and Ru–N(1) distances (from 2.081(2) to 2.10(2) Å) are comparable to those reported for other arene ruthenium complexes containing azobenzene ligands.<sup>16,20,27</sup> It should be noted that the (*E*)-azo ligands do not adopt a planar geometry after coordination. The angles between the planes of



Scheme 4. Synthesis of Fluorinated Ligand 11 and Complex 12



Scheme 5. Synthesis of Benzene and Hexamethylbenzene Complexes 13 and 14



the two aromatic groups of azobenzene are nearly identical in compounds 4 and 7 ( $\theta = 57.38$  and  $54.96^\circ$ , respectively), while this value is higher in 9 ( $68.27^\circ$ ) and significantly reduced in 14 ( $30.83^\circ$ ). Interestingly, the X-ray structure of 9 shows a component of disorder around the isopropyl group of the *p*-cymene moiety.

The  $^1\text{H}$  NMR spectra of 4, 7, 9, and 12–14 in  $\text{CDCl}_3$  revealed well-defined signals corresponding to the azobenzene ligand, while signals related to the *p*-cymene moiety showed great differences in complexes 4, 7, 9, and 12. In 4 and 7, *p*-cymene exhibits characteristic signals for aromatic protons: two

Table 1. Selected Bond Lengths (Å) and angles (deg) for Complexes 4, 7, 9, and 14

	4	7	9	14
Ru–N(1)	2.081(2)	2.090(5)	2.093(2)	2.10(2)
Ru–N(3)	2.101(2)	2.104(5)	2.132(3)	2.12(1)
Ru–Cl(1)	2.3993(8)	2.405(2)	2.398(1)	2.404(5)
Ru–cent <sup>a</sup>	1.703	1.714	1.702	1.710
N(1)–N(2)	1.258(3)	1.255(6)	1.263(3)	1.28(3)
N(3)–S(1)	1.618(2)	1.631(6)	1.590(3)	1.63(2)
N(3)–Ru–Cl(1)	85.65(7)	85.6(1)	85.06(8)	88.7(4)
N(3)–Ru–N(1)	77.57(9)	78.0(2)	78.0(1)	77.4(6)
N(1)–Ru–Cl(1)	86.46(6)	88.7(1)	87.32(8)	94.5(5)
$\theta^b$	57.38	54.96	68.27	30.83

<sup>a</sup>cent = centroid of arene moiety. <sup>b</sup> $\theta$  = angle between the planes of the two aromatic rings of the azobenzene ligand.

doublets in the range 5.43–5.33 and 5.05–5.02 ppm and two broad signals at 6.32–6.20 and 3.74–3.51 ppm, as a consequence of the strong ring current effect exerted by the azobenzene ligand (see Figure 6, the Supporting Information, and the discussion above), while the *i*-Pr group appears as a septuplet at 2.67–2.56 ppm and two doublets at 1.08–1.07 and 0.89–0.87 ppm and the Me group appears as a singlet at 2.15–2.11 ppm. The  $^1\text{H}$  NMR spectrum of 12 shows broad signals corresponding to aromatic protons above 6.5 ppm (1H), around 5.5 ppm (2H), and around 3.7 ppm (several signals corresponding to 1H). The *i*-Pr group appears as broad signals at 2.83, 1.19, and 0.87 ppm, and the Me group shows a broad signal at 1.99 ppm. The pattern exhibited by *p*-cymene in 9 is slightly different, with seven broad signals appearing between 6.03 and 3.98 ppm (aromatic protons), around 2.50 and 1.00 ppm (*i*-Pr group), and in the range 2.39–2.08 ppm (Me group). The observation of such broad signals for 12 and 9 presumably indicates their existence as slowly interconverting conformers in solution, consistent with the disorder observed around the *i*-Pr group of 9 in the solid state. The signals of the arene group of 13 and 14 appear as singlets at 5.48 and 1.83 ppm, respectively.

The spectroscopic properties of the synthesized complexes in MeCN were compared and are summarized in Table 2. Compounds 4, 7, 9, 12, and 13 displayed similar absorption spectra (Figure 4 and the Supporting Information), with two bands around 314–319 nm and 390–454 nm that can be assigned to the  $\pi \rightarrow \pi^*$  intraligand transition and one band around 514–586 nm with a lower extinction coefficient that

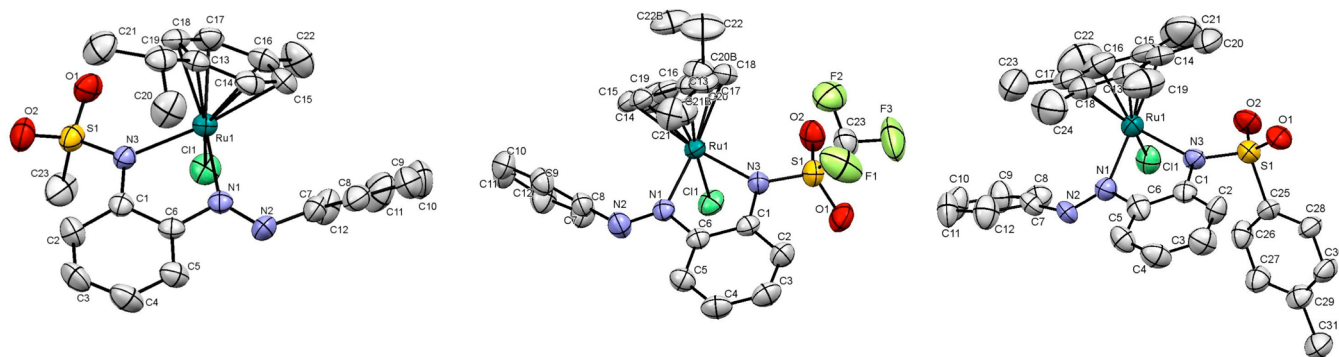
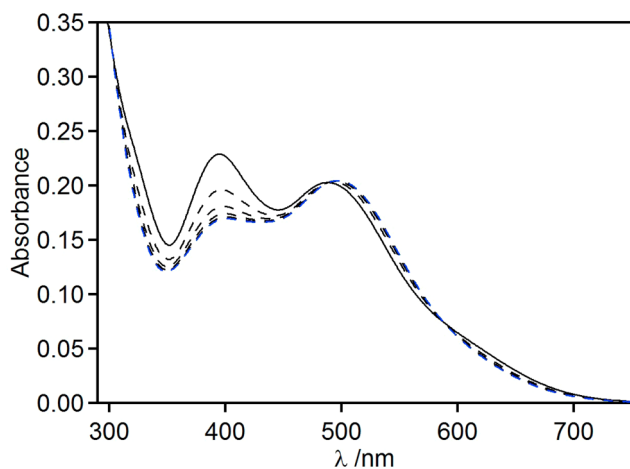


Figure 8. ORTEP representation (thermal ellipsoids drawn at the 50% probability level) of complexes 7 (left), 9 (middle), and 14 (right) with the atom-numbering scheme. The hydrogen atoms and solvent molecule (for 14:  $\text{CH}_2\text{Cl}_2$ ) have been removed for clarity.

**Table 2. Electronic Spectral Data and Transition Assignment for Complexes 4–14 in CH<sub>3</sub>CN**

compound	$\lambda$ /nm	$\epsilon$ /L mol <sup>-1</sup> cm <sup>-1</sup>	transition
4	319	9574 $\pm$ 21	$\pi \rightarrow \pi^*$
	421	6850 $\pm$ 24	$\pi \rightarrow \pi^*$
	566	2740 $\pm$ 14	MLCT
7	315	7729 $\pm$ 28	$\pi \rightarrow \pi^*$
	400	5516 $\pm$ 15	$\pi \rightarrow \pi^*$
	560	2231 $\pm$ 27	MLCT
9	314	7395 $\pm$ 88	$\pi \rightarrow \pi^*$
	390	5437 $\pm$ 60	$\pi \rightarrow \pi^*$
	514	1621 $\pm$ 50	MLCT
12	317	7400 $\pm$ 28	$\pi \rightarrow \pi^*$
	454	5448 $\pm$ 53	$\pi \rightarrow \pi^*$
	586	1847 $\pm$ 34	MLCT
13	316	8133 $\pm$ 11	$\pi \rightarrow \pi^*$
	444	5022 $\pm$ 26	$\pi \rightarrow \pi^*$
	556	2604 $\pm$ 45	MLCT
14	319	6842 $\pm$ 21	$\pi \rightarrow \pi^*$
	394	8557 $\pm$ 38	$\pi \rightarrow \pi^*$
	485	5872 $\pm$ 15	$\pi \rightarrow \pi^*$
	617	1719 $\pm$ 40	MLCT

can be assigned to the MLCT (metal–ligand charge transfer) transition from the 4d orbitals of Ru(II) to the empty  $\pi^*$  ligand orbitals (Table 2). As a plausible consequence of the singular geometry of **14** in comparison to other complexes, this compound exhibited a notably different pattern with three intense bands at 319, 394, and 485 nm assigned to  $\pi \rightarrow \pi^*$  intraligand transitions and a broad band around 617 nm corresponding to an MLCT transition (Figure 9). As previously



**Figure 9.** Absorption spectrum of ruthenium complex (E)-**14** in MeCN ( $C = 30 \mu\text{M}$ ) at 25 °C (black solid line) and its stepwise evolution upon 5 s irradiation pulses at 406 nm with  $P = 9 \text{ mW cm}^{-2}$  (black dashed lines). The blue dashed line corresponds to the PSS.

described for **4**, irradiation at 406 nm of complexes **7**, **9**, and **12–14** in MeCN induced photoisomerization of the ligand, as revealed by a decrease in the absorption band at 390–454 nm and an increase around 500–550 nm (Figure 9 and the Supporting Information).

**Solvent Effects on Thermal  $Z \rightarrow E$  Isomerization Rates of Complexes.** In order to assess the influence of solvent on the isomerization properties of the synthesized complexes, solutions of **4**, **7**, **9**, and **12–14** in solvents with varying

polarities (toluene, THF, CH<sub>2</sub>Cl<sub>2</sub>, acetone, MeCN, and EtOH) were prepared. Irradiation at 406 nm cleanly triggered  $E \rightarrow Z$  photoisomerization; then the half-life of the  $Z$  isomer (rate of thermal back-reaction) was determined by monitoring the evolution of absorbance at the appropriate wavelength (see the Supporting Information for details). The results are reported in Table 3. For most complexes studied,  $t_{1/2}(Z)$  increases with increasing solvent polarity (as evaluated by the empirical polarity scale  $E_T^N$ ),<sup>60</sup> ranging from 0.66 to 3.68 min in toluene ( $E_T^N = 0.099$ ) to 3.48 to 33.6 min in EtOH ( $E_T^N = 0.654$ ). It is worth noting the case of CH<sub>2</sub>Cl<sub>2</sub> ( $E_T^N = 0.309$ ), which, although slightly less polar than acetone ( $E_T^N = 0.355$ ), results in longer  $t_{1/2}(Z)$  values. The general trends observed can be understood in term of a better solvation of  $Z$  complexes (exhibiting a higher permanent dipole than  $E$  isomers) in polar solvents, thus increasing their thermal stability and consequently the  $t_{1/2}(Z)$  values.<sup>51,61,62</sup>

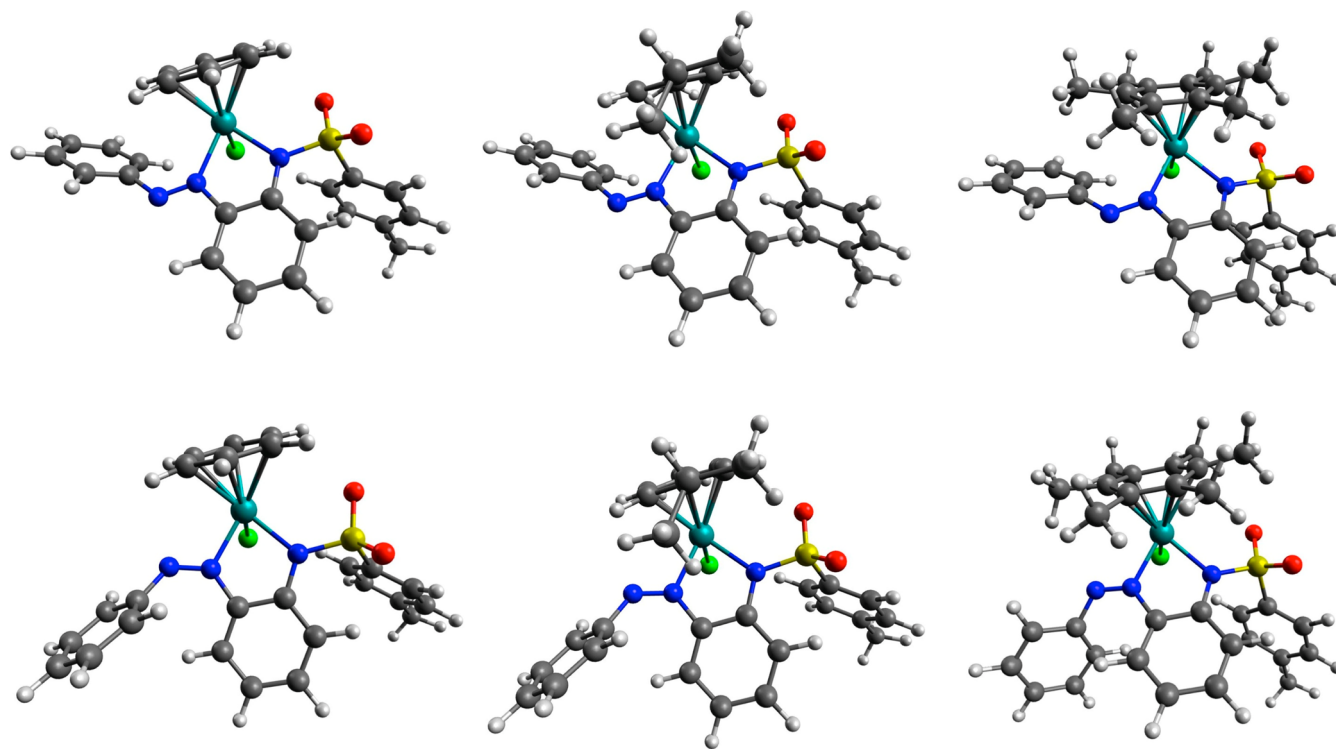
While *o*-fluoroazobenzenes are well-known to exist as very long lived  $Z$  isomers (with half-lives reaching more than 2 years),<sup>51,52</sup> the  $t_{1/2}(Z)$  value for **12** is on the time scale of several minutes as for other Ru complexes. Although the factors responsible for such a behavior could not yet be precisely identified, it is likely that coordination of azobenzene to the metal center affected the  $\pi$ -conjugation structure and the increment in the dipole moment.<sup>37</sup> In addition, the conformational change of the azobenzene ligand associated with Ru coordination led to an increase in the angle between the planes of the two aromatic rings (Table 1) which might facilitate the  $Z \rightarrow E$  thermal isomerization. Interestingly, the nature of the sulfonamide group exerts a significant effect on the rate of  $Z \rightarrow E$  thermal isomerization, with (Z)-**9** (Tf group) showing a longer half-life than (Z)-**4** (Ts group) and (Z)-**7** (Ms group). The Hammett constant  $F$ , recognized as a good quantification of the inductive withdrawing effect of a substituent, parallels this observation: the most electron withdrawing group Tf ( $F = 0.74$ )<sup>63</sup> indeed shows a longer  $t_{1/2}(Z)$  value than Ts ( $F = 0.55$ )<sup>64</sup> and Ms ( $F = 0.54$ )<sup>35</sup>. Finally, the most striking aspect concerning the structure–property relationship in our complexes is the influence of the arene group on the isomerization.

A comparison of **4**, **13**, and **14** clearly revealed a strong effect of the presence of the hexamethylbenzene ligand on the half-life of the  $Z$  isomer. Indeed, while **4** and **13** exhibited similar  $t_{1/2}(Z)$  values ranging from 1.50 to 7.29 min depending on the solvent,  $t_{1/2}(Z)$  for **14** varied between 2.33 and 33.6 min. In order to understand the origin of such a difference, the geometry of both  $E$  and  $Z$  isomers of complexes **4**, **13**, and **14** was optimized by DFT calculations using Gaussian 09<sup>65</sup> at the B3LYP/6-31G\*\*(d,p);LanL2DZ[Ru] level and the CPCM model for MeCN (Figure 10). All three  $E$  isomers exhibit similar geometries, with angles between the planes of the two aromatic rings of the azobenzene ligand ( $\theta$ ) of 55.07, 50.79, and 33.49° for **4**, **13**, and **14**, respectively. These results are in good agreement with the  $\theta$  values determined for **4** (57.38°) and **14** (30.83°) in the solid state by X-ray analysis (see Table 1). Interestingly, although (Z)-**4** and (Z)-**13** exhibit similar geometries ( $\theta = 64.26$  and 62.17°, respectively), the relative orientation of phenyl rings in azobenzene (Z)-**14** is reversed, leading to a  $\theta$  value of  $-64.62^\circ$ . Such observation is presumably the result of two phenomena: (i) steric interactions exerted by the methyl groups of the hmbz ligand on the phenyl ring of azobenzene and (ii) a change in the polarity of  $E$  and  $Z$  complexes and their HOMO energy as a consequence of electron enrichment of the metal center by the hmbz ligand.

**Table 3.** Half-Lives ( $t_{1/2}$ , min) of Z Isomers of Complexes 4–14 in Various Solvents (Ranked by Order of Increasing Polarity Parameter  $E_T^N$ )<sup>a</sup>

entry	solvent	$E_T^N$	4	7	9	12	13	14
1	toluene	0.099	1.50 ± 0.01	0.66 ± 0.01	3.68 ± 0.01	1.21 ± 0.01	2.26 ± 0.03	2.33 ± 0.02
2	THF	0.207	2.65 ± 0.01	1.12 ± 0.01	5.05 ± 0.02	2.38 ± 0.01	2.63 ± 0.09	3.78 ± 0.03
3	CH <sub>2</sub> Cl <sub>2</sub>	0.309	5.55 ± 0.02	2.85 ± 0.02	6.51 ± 0.01	7.02 ± 0.10	4.82 ± 0.57	18.3 ± 0.1
4	acetone	0.355	5.44 ± 0.02	2.26 ± 0.01	5.67 ± 0.01	5.23 ± 0.02	4.28 ± 0.88	10.9 ± 0.1
5	MeCN	0.460	6.46 ± 0.31	2.33 ± 0.01	10.1 ± 0.1	8.11 ± 0.03	2.26 ± 0.36	26.5 ± 0.2
6	EtOH	0.654	7.29 ± 0.05	3.48 ± 0.02	n.d. <sup>b</sup>	11.8 ± 0.5	6.45 ± 0.25	33.6 ± 0.3

<sup>a</sup>Z isomers were formed by irradiation at 406 nm ( $P = 9 \text{ mW cm}^{-2}$ ) for 20 s, and then thermal back-isomerization was followed by monitoring UV/vis absorption in the dark at 25 °C. <sup>b</sup>n.d.: not determined (unstable in EtOH).

**Figure 10.** DFT-optimized geometries for E (top) and Z isomers (bottom) of complexes 13 (left), 4 (middle), and 14 (right).

## CONCLUSION

A novel series of arene ruthenium complexes containing *o*-sulfonamide azobenzene ligands was synthesized and characterized. The unusual coordination pattern exhibited by the N=N bond of the azobenzene ligand, which was found to be exocyclic, allowed the preservation of its photoisomerization properties, thus leading to photoswitchable organometallic complexes. In comparison to uncoordinated azobenzene ligands, the corresponding Ru complexes favored the  $Z \rightarrow E$  thermal isomerization. The influence of solvent and structural parameters, such as substituents on the phenyl ring of azobenzene and the nature of the sulfonamide group and arene ligand, on the rate of thermal  $Z \rightarrow E$  back-isomerization was investigated, and the presence of hexamethylbenzene group on ruthenium was found to significantly increase the half-life of the corresponding Z isomer. On the basis of DFT calculations, this effect was rationalized by steric interactions between the arene ligand and the phenyl ring of azobenzene. With these novel photoswitchable organometallic complexes with well-defined properties in hand, our current efforts are focused on the study of their reactivity.

## EXPERIMENTAL SECTION

**General Procedures.** Unless otherwise stated, all reagents were used as received without further purification. Manipulations under anhydrous conditions were carried out under an atmosphere of argon in dried glassware. Solvents were dried with a mBraun MB-SPS-800 purification system. <sup>1</sup>H and <sup>13</sup>C{<sup>1</sup>H} NMR spectra were recorded on a JEOL 400 spectrometer and referenced to the resonances of the solvent residual peak. Infrared (IR) spectra were recorded with a Nicolet Nexus FT-IR spectrometer equipped with an ATR-Germanium unit and are reported as wavenumbers (cm<sup>-1</sup>). Melting points were determined using a Kofler bench. High-resolution mass spectra (HRMS) were obtained on a Bruker maXis Q-TOF mass spectrometer by the “Fédération de Recherche” ICOA/CBM (FR2708) platform. Elemental analyses were carried out by the Laboratory for Microanalysis at ICSN (Gif-sur-Yvette, France). Crystals suitable for X-ray analysis were obtained either by slow evaporation of a solution of the complexes in CH<sub>2</sub>Cl<sub>2</sub> or by slow vapor diffusion of petroleum ether in a solution of the complexes in CH<sub>2</sub>Cl<sub>2</sub>.

**Spectroscopic Measurements.** Acetonitrile, acetone, dichloromethane, ethanol, toluene, and THF used for absorption measurements were of spectrometric grade. Dichloromethane was passed through a neutral alumina column prior to use to avoid any acidic catalysis. UV/vis absorption spectra were recorded on a Cary5000 spectrophotometer from Agilent Technologies. Photoisomerization



was induced by a continuous irradiation Hg/Xe lamp (Hamamatsu, LC6 Lightningcure, 200 W) equipped with narrow-band interference filters of appropriate wavelengths (Semrock FF01-315/15-25 for  $\lambda_{\text{irr}}$  315 nm; FF01-406/15-25 for  $\lambda_{\text{irr}}$  406 nm). The irradiation power was measured using a photodiode from Ophir (PD300-UV).

**N-(2-Nitrosophenyl)-4-methylbenzenesulfonamide (2).** To a solution of **1**<sup>49</sup> (100 mg, 0.362 mmol) in  $\text{CH}_2\text{Cl}_2$  (5 mL) was added dropwise a solution of oxone (281 mg, 0.457 mmol, 1.2 equiv) in 5 mL of  $\text{H}_2\text{O}$ . The resulting mixture was vigorously stirred at room temperature for 24 h. The layers were separated, and the aqueous layer was extracted with  $\text{CH}_2\text{Cl}_2$  ( $2 \times 5$  mL). The organic layers were combined, washed with brine, dried over anhydrous sodium sulfate, and evaporated under vacuum to afford **2** (99 mg, 0.36 mmol, 94%): green crystalline solid;  $R_f = 0.35$  (petroleum ether/ethyl acetate 8/2); mp 135 °C; IR 3662, 3227, 2986, 2902, 1624, 1597, 1492, 1320, 1164, 1127, 915, 819, 763, 684  $\text{cm}^{-1}$ ;  $^1\text{H}$  NMR (400 MHz,  $(\text{CD}_3)_2\text{CO}$ )  $\delta$  10.81 (br s, 1 H), 7.93 (d,  $J = 8.2$  Hz, 1H), 7.85 (d,  $J = 8.2$  Hz, 2H), 7.76 (m, 1H), 7.33 (d,  $J = 8.2$  Hz, 2H), 7.15 (t,  $J = 7.6$  Hz, 1H), 6.71 (d,  $J = 7.3$  Hz, 1H), 2.33 (s, 3H);  $^{13}\text{C}\{^1\text{H}\}$  NMR (100 MHz,  $(\text{CD}_3)_2\text{CO}$ )  $\delta$  158.1, 145.5, 139.7, 139.5, 137.7, 130.8, 128.4, 124.3, 122.3, 114.0, 21.5; HRMS (ESI) calcd for  $\text{C}_{13}\text{H}_{12}\text{N}_3\text{O}_3\text{SK}^+ [\text{M} + \text{K}]^+$   $m/z$  315.0200, found  $m/z$  315.0198.

**(E)-2-(4-Methylphenylsulfonamido)azobenzene (3).**<sup>66</sup> To a solution of aniline (100  $\mu\text{L}$ , 1.10 mmol) in toluene (20 mL) were added acetic acid (260  $\mu\text{L}$ , 4.40 mmol, 4 equiv) and **2** (305 mg, 1.10 mmol, 1 equiv). The resulting mixture was stirred under reflux for 48 h, and  $\text{H}_2\text{O}$  (20 mL) was added. The layers were separated, and the aqueous layer was extracted with toluene ( $2 \times 10$  mL). The organic layers were combined, washed with a saturated aqueous solution of  $\text{NaHCO}_3$  (10 mL), dried over anhydrous sodium sulfate, and evaporated under vacuum. The crude product was purified by flash chromatography (silica gel-petroleum ether/ethyl acetate 8/2) to afford **3** (350 mg, 1.00 mmol, 90%): orange crystalline solid;  $R_f = 0.30$  (petroleum ether/ethyl acetate 8/2); mp 105 °C (lit.<sup>66</sup> mp 129 °C); IR 3251, 1597, 1478, 1389, 1336, 1167, 1092, 911, 772, 693  $\text{cm}^{-1}$ ;  $^1\text{H}$  NMR (400 MHz,  $(\text{CD}_3)_2\text{CO}$ )  $\delta$  9.71 (br s, 1H), 7.89 (m, 2H), 7.76 (d,  $J = 9.2$  Hz, 1H), 7.69–7.66 (m, 3H), 7.60–7.58 (m, 3H), 7.53 (t,  $J = 7.8$  Hz, 1H), 7.25 (t,  $J = 7.8$  Hz, 1H), 7.16 (d,  $J = 7.8$  Hz, 2H), 2.22 (s, 3H);  $^{13}\text{C}\{^1\text{H}\}$  NMR (100 MHz,  $(\text{CD}_3)_2\text{CO}$ )  $\delta$  153.1, 144.7, 142.9, 137.6, 136.7, 133.3, 132.5, 130.3, 130.1, 127.9, 125.9, 123.9, 123.5, 119.8, 21.3.

**Complex 4.** To a solution of **3** (80 mg, 0.23 mmol) in 10 mL of MeOH were added  $\text{Et}_3\text{N}$  (62  $\mu\text{L}$ , 0.46 mmol) and  $[\text{Ru}(\text{p-cym})\text{Cl}_2]_2$  (70 mg, 0.11 mmol). After the mixture was stirred for 24 h, the precipitate was filtered and washed with  $\text{Et}_2\text{O}$  to afford **4** (112 mg, 0.180 mmol, 78%): brown powder;  $R_f = 0.73$  ( $\text{CH}_2\text{Cl}_2/\text{MeOH}$  95/5); mp 244 °C; IR 2969, 1596, 1474, 1305, 1142, 1082, 932, 851, 763, 697  $\text{cm}^{-1}$ ;  $^1\text{H}$  NMR (400 MHz,  $\text{CDCl}_3$ )  $\delta$  8.09 (d,  $J = 8.2$  Hz, 2H), 7.86 (m, 3H), 7.64 (t,  $J = 7.8$  Hz, 2H), 7.52 (m, 1H), 7.38 (d,  $J = 8.7$  Hz, 1H), 7.15 (d,  $J = 8.2$  Hz, 2H), 7.04 (t,  $J = 8.4$  Hz, 1H), 6.60 (t,  $J = 7.6$  Hz, 1H), 6.32 (br s, 1H), 5.43 (d,  $J = 6.0$  Hz, 1H), 5.05 (d,  $J = 5.5$  Hz, 1H), 3.74 (br s, 1H), 2.67 (sept,  $J = 6.9$  Hz, 1H), 2.31 (s, 3H), 2.15 (s, 3H), 1.08 (d,  $J = 6.9$  Hz, 3H), 0.87 (d,  $J = 6.9$  Hz, 3H);  $^{13}\text{C}\{^1\text{H}\}$  NMR (100 MHz,  $\text{CDCl}_3$ )  $\delta$  156.0, 151.6, 148.5, 142.1, 137.9, 133.3, 129.3, 128.9, 128.7, 122.5, 119.6, 119.0, 118.4, 82.9, 82.5, 31.0, 23.6, 21.6, 21.2, 19.3; HRMS (ESI) calcd for  $\text{C}_{29}\text{H}_{30}\text{N}_3\text{O}_2\text{RuS}^+ [\text{M} - \text{Cl}]^+$   $m/z$  586.1104, found  $m/z$  586.1106. Anal. Calcd for  $\text{C}_{29}\text{H}_{30}\text{N}_3\text{O}_2\text{RuS}$ , C, 56.08; H, 4.87; N, 6.76. Found: C, 56.11; H, 4.95; N, 6.61.

**(E)-2-(Methanesulfonamido)azobenzene (6).** To a solution of **5**<sup>53</sup> (50 mg, 0.25 mmol) in pyridine (5 mL) was added methanesulfonyl chloride (22  $\mu\text{L}$ , 0.28 mmol, 1.1 equiv). Stirring at room temperature for 12 h was followed by addition of another portion of methanesulfonyl chloride (22  $\mu\text{L}$ , 0.28 mmol, 1.1 equiv). After completion of the reaction, the mixture was evaporated to dryness.  $\text{CH}_2\text{Cl}_2$  (20 mL) and  $\text{H}_2\text{O}$  (20 mL) were added, the layers were separated, and the aqueous layer was extracted with  $\text{CH}_2\text{Cl}_2$  ( $3 \times 10$  mL). The organic layers were combined, washed with a saturated aqueous solution of  $\text{NH}_4\text{Cl}$  (10 mL), dried over anhydrous sodium sulfate, and evaporated under vacuum. The crude product was purified by flash chromatography (silica gel, petroleum ether/ethyl acetate 8/

2) to afford **6** (57 mg, 0.21 mmol, 82%): orange crystalline solid;  $R_f = 0.34$  (petroleum ether/ethyl acetate 8/2); mp 100 °C; IR 3270, 1595, 1484, 1375, 1335, 1166, 1152, 971, 773, 732, 690  $\text{cm}^{-1}$ ;  $^1\text{H}$  NMR (400 MHz,  $(\text{CD}_3)_2\text{CO}$ )  $\delta$  9.52 (br s, 1H), 8.00 (m, 2H), 7.87 (dd,  $J = 8.0$ , 1.6 Hz, 1H), 7.79 (m, 1H), 7.62–7.56 (m, 4H), 7.31 (ddd,  $J = 8.4$ , 7.2, 1.4 Hz, 1H), 3.15 (s, 3H);  $^{13}\text{C}\{^1\text{H}\}$  NMR (100 MHz,  $(\text{CD}_3)_2\text{CO}$ )  $\delta$  153.2, 141.8, 137.3, 133.7, 132.6, 130.2, 125.1, 123.9, 121.4, 120.4, 40.2; HRMS (ESI) calcd for  $\text{C}_{13}\text{H}_{11}\text{N}_3\text{O}_2\text{SNa}^+ [\text{M} + \text{Na}]^+$   $m/z$  298.0626, found  $m/z$  298.0629.

**Complex 7.** To a solution of **6** (19 mg, 0.066 mmol) in 4 mL of MeOH were added  $\text{Et}_3\text{N}$  (18  $\mu\text{L}$ , 0.13 mmol) and  $[\text{Ru}(\text{p-cym})\text{Cl}_2]_2$  (20 mg, 0.033 mmol). After it was stirred for 24 h, the mixture was evaporated to dryness and the product was purified by flash chromatography (silica gel,  $\text{CH}_2\text{Cl}_2/\text{MeOH}$  250/2 to 250/4) to afford **7** (23 mg, 0.042 mmol, 63%): black powder;  $R_f = 0.58$  ( $\text{CH}_2\text{Cl}_2/\text{MeOH}$  95/5); mp 189 °C; IR 3477, 1593, 1468, 1300, 1241, 1126, 960, 926, 845, 733, 679  $\text{cm}^{-1}$ ;  $^1\text{H}$  NMR (400 MHz,  $\text{CDCl}_3$ )  $\delta$  8.09 (d,  $J = 8.7$  Hz, 1H), 7.95 (dd,  $J = 8.5$ , 1.1 Hz, 1H), 7.75 (d,  $J = 7.8$  Hz, 2H), 7.61 (t,  $J = 7.8$  Hz, 2H), 7.50 (m, 1H), 7.34 (m, 1H), 6.76 (m, 1H), 6.20 (br s, 1H), 5.33 (d,  $J = 6.0$  Hz, 1H), 5.02 (d,  $J = 5.5$  Hz, 1H), 3.51 (br s, 1H), 3.12 (s, 3H), 2.56 (sept,  $J = 6.9$  Hz, 1H), 2.11 (s, 3H), 1.07 (d,  $J = 6.9$  Hz, 3H), 0.89 (d,  $J = 6.9$  Hz, 3H);  $^{13}\text{C}\{^1\text{H}\}$  NMR (100 MHz,  $\text{CDCl}_3$ )  $\delta$  156.4, 152.4, 149.3, 134.1, 129.0, 128.6, 122.1, 119.8, 119.0, 83.0, 82.8, 41.0, 31.0, 23.3, 21.5, 19.2; HRMS (ESI) calcd for  $\text{C}_{23}\text{H}_{27}\text{N}_3\text{O}_2\text{RuS}^+ [\text{M} - \text{Cl}]^+$   $m/z$  510.0789, found  $m/z$  510.0789. Anal. Calcd for  $\text{C}_{23}\text{H}_{27}\text{N}_3\text{O}_2\text{RuS}$ , C, 50.68; H, 4.81; N, 7.71. Found: C, 50.35; H, 4.73; N, 7.34.

**(E)-2-(Trifluoromethanesulfonamido)azobenzene (8).** To a solution of **5** (208 mg, 1.05 mmol) in dry  $\text{CH}_2\text{Cl}_2$  (20 mL) under argon was added trifluoromethanesulfonic acid (196  $\mu\text{L}$ , 1.16 mmol, 1.1 equiv). The mixture was stirred at room temperature for 10 min before addition of  $\text{H}_2\text{O}$  (20 mL). The layers were separated, and the aqueous layer was extracted with  $\text{CH}_2\text{Cl}_2$  ( $3 \times 20$  mL). The organic layers were combined, washed with brine (10 mL), dried over anhydrous sodium sulfate, and finally evaporated under vacuum. **8** (325 mg, 94%) was used without further purification. A small portion for analysis was purified by flash chromatography (silica gel, petroleum ether/ethyl acetate 98/2): orange crystalline solid;  $R_f = 0.58$  (petroleum ether/ethyl acetate 8/2); mp 76 °C; IR 3264, 1597, 1485, 1415, 1214, 1193, 1140, 957, 770, 684  $\text{cm}^{-1}$ ;  $^1\text{H}$  NMR (400 MHz,  $(\text{CD}_3)_2\text{CO}$ )  $\delta$  10.71 (br s, 1H), 8.03 (dd,  $J = 7.8$ , 1.8 Hz, 2H), 7.86 (dd,  $J = 8.0$ , 1.6 Hz, 1H), 7.75 (m, 1H), 7.67 (m, 1H), 7.62–7.60 (m, 3H), 7.53 (m, 1H);  $^{13}\text{C}\{^1\text{H}\}$  NMR (100 MHz,  $(\text{CD}_3)_2\text{CO}$ )  $\delta$  153.4, 146.0, 134.5, 133.3, 132.9, 130.2, 128.9, 127.1, 124.2, 117.8; HRMS (ESI) calcd for  $\text{C}_{13}\text{H}_{11}\text{F}_3\text{N}_3\text{O}_2\text{S}^+ [\text{M} + \text{H}]^+$   $m/z$  330.0519, found  $m/z$  330.0519.

**Complex 9.** A solution of **8** (108 mg, 0.328 mmol) in 10 mL of MeOH and  $[\text{Ru}(\text{p-cym})\text{Cl}_2]_2$  (100 mg, 0.215 mmol) was stirred for 48 h and evaporated to dryness. The product was purified by flash chromatography (silica gel,  $\text{CH}_2\text{Cl}_2/\text{MeOH}$  250/2 to 250/5) to afford **9** (58 mg, 0.097 mmol, 29%): dark red powder;  $R_f = 0.77$  ( $\text{CH}_2\text{Cl}_2/\text{MeOH}$  95/5); mp 245 °C; IR 3057, 1598, 1476, 1353, 1203, 1179, 1162, 1134, 949, 838, 767, 694  $\text{cm}^{-1}$ ;  $^1\text{H}$  NMR (400 MHz,  $\text{CDCl}_3$ )  $\delta$  8.11–7.77 (br s, 1H), 7.97 (d,  $J = 8.7$  Hz, 1H), 7.86 (d,  $J = 7.8$  Hz, 2H), 7.65 (m, 2H), 7.54 (m, 1H), 7.37 (ddd,  $J = 8.6$ , 7.0, 1.4 Hz, 1H), 6.91 (m, 1H), 6.03–3.98 (7 br s, 1H), 2.49 (br s, 1H), 2.39–2.08 (m, 3H), 1.07–0.83 (m, 6H);  $^{13}\text{C}\{^1\text{H}\}$  NMR (100 MHz,  $\text{CDCl}_3$ )  $\delta$  155.8 (br), 149.6, 149.1, 133.7, 129.3, 129.2, 122.1, 121.9, 120.7 (br), 118.7, 108.5 (br), 102.5 (br), 92.1 (br), 89.0 (br), 86.0 (br), 85.1 (br), 83.5–82.5 (br), 66.0, 31.1, 30.0, 22.9–21.6 (br), 19.2, 15.4; HRMS (ESI) calcd for  $\text{C}_{23}\text{H}_{23}\text{F}_3\text{N}_3\text{O}_2\text{RuS}^+ [\text{M} - \text{Cl}]^+$   $m/z$  564.0507, found  $m/z$  564.0519. Anal. Calcd for  $\text{C}_{23}\text{H}_{23}\text{F}_3\text{N}_3\text{O}_2\text{RuS}$ , C, 46.12; H, 3.87; N, 7.01. Found: C, 46.36; H, 4.13; N, 7.05.

**2,6-Difluoroazobenzene (10).** To a solution of 2,6-difluoroaniline (500  $\mu\text{L}$ , 4.65 mmol) in  $\text{CH}_2\text{Cl}_2$  (15 mL) was added dropwise a solution of oxone (5.71 g, 9.29 mmol, 2 equiv) in 15 mL of  $\text{H}_2\text{O}$ . The resulting mixture was vigorously stirred at room temperature for 15 h. The layers were separated, and the aqueous layer was extracted with  $\text{CH}_2\text{Cl}_2$  ( $2 \times 5$  mL). The organic layers were combined, washed with a saturated aqueous solution of  $\text{NaHCO}_3$  (10



mL), dried over anhydrous sodium sulfate, and evaporated under vacuum to afford **10** (660 mg, 4.61 mmol, 99%): light brown powder;  $R_f$  = 0.55 (petroleum ether/ethyl acetate 8/2); mp 119 °C; IR 3662, 3225, 2986, 2901, 1608, 1478, 1283, 1163, 1086, 1019, 914, 788  $\text{cm}^{-1}$ ;  $^1\text{H}$  NMR (400 MHz,  $(\text{CD}_3)_2\text{CO}$ )  $\delta$  7.92 (m, 1H), 7.37 (t,  $J$  = 8.9 Hz, 2H);  $^{13}\text{C}\{^1\text{H}\}$  NMR (100 MHz,  $(\text{CD}_3)_2\text{CO}$ )  $\delta$  154.2 (d,  $J$  = 267 Hz), 139.6 (t,  $J$  = 11.4 Hz), 114.1 (d,  $J$  = 23.8 Hz).

**(E)-2-(4-Methylphenylsulfonamido)-2',6'-difluoroazobenzene (11).** To a solution of **1** (92 mg, 0.35 mmol) in acetic acid (5 mL) was added **10** (50 mg, 0.35 mmol, 1 equiv). The resulting mixture was stirred under reflux for 16 h and evaporated to dryness under vacuum. The crude product was purified by flash chromatography (silica gel, petroleum ether/ethyl acetate 9/1) to afford **11** (33 mg, 0.085 mmol, 24%): orange crystalline solid;  $R_f$  = 0.39 (petroleum ether/ethyl acetate 8/2); mp 140 °C; IR 3299, 1613, 1594, 1477, 1390, 1338, 1165, 1092, 1028, 926, 759  $\text{cm}^{-1}$ ;  $^1\text{H}$  NMR (400 MHz,  $\text{CDCl}_3$ )  $\delta$  9.20 (s, 1H); 7.79 (d,  $J$  = 8.2 Hz, 1H), 7.72–7.69 (m, 3H), 7.44 (m, 1H), 7.40 (ddd,  $J$  = 8.5, 6.0, 2.5 Hz, 1H), 7.17–7.06 (m, 5H), 2.33 (s, 3H);  $^{13}\text{C}\{^1\text{H}\}$  NMR (100 MHz,  $\text{CDCl}_3$ )  $\delta$  156.3 (d,  $J$  = 259 Hz), 144.2, 141.0, 136.2, 136.1, 133.9, 131.4 (t,  $J$  = 10.5 Hz), 129.8, 127.4, 124.2, 119.9, 119.8, 112.9, 21.6; HRMS (ESI) calcd for  $\text{C}_{19}\text{H}_{15}\text{F}_2\text{N}_3\text{O}_2\text{SNa}^+ [\text{M} + \text{Na}]^+ m/z$  410.0751, found  $m/z$  410.0748.

**Complex 12.** To a solution of **11** (97 mg, 0.26 mmol) in 10 mL of MeOH were added  $\text{Et}_3\text{N}$  (70  $\mu\text{L}$ , 0.52 mmol) and  $[\text{Ru}(p\text{-cym})\text{Cl}_2]_2$  (80 mg, 0.13 mmol). After it was stirred for 24 h, the mixture was evaporated to dryness and the product was purified by flash chromatography (silica gel,  $\text{CH}_2\text{Cl}_2/\text{MeOH}$  250/3) to afford **12** (93 mg, 0.14 mmol, 57%): black powder;  $R_f$  = 0.65 ( $\text{CH}_2\text{Cl}_2/\text{MeOH}$  95/5); mp 245 °C; IR 3738, 2967, 1712, 1595, 1469, 1400, 1308, 1245, 1139, 1081, 1007, 924, 849, 787  $\text{cm}^{-1}$ ;  $^1\text{H}$  NMR (400 MHz,  $\text{CDCl}_3$ )  $\delta$  8.08 (d,  $J$  = 7.8 Hz, 2H), 7.69 (d,  $J$  = 8.2 Hz, 1H), 7.43–7.37 (m, 2H), 7.20–7.05 (m, 5H), 6.91 (m, 1H), 6.60 (t,  $J$  = 7.8 Hz, 1H), 5.51–5.46 (m, 2H), 3.66 (br s, 1H), 2.83 (m, 1H), 2.27 (s, 3H), 1.99 (s, 3H), 1.19 (br s, 3H), 0.87 (br s, 3H);  $^{13}\text{C}\{^1\text{H}\}$  NMR (100 MHz,  $\text{CDCl}_3$ )  $\delta$  151.0 (d,  $J$  = 237 Hz), 142.2, 137.4, 134.2, 133.6, 129.3, 129.0, 128.6 (t,  $J$  = 91 Hz), 119.3, 119.2, 118.8, 111.7 (br), 100.1, 97.3, 83.2, 81.8, 78.7, 53.6, 31.2, 31.1, 24.5, 21.6, 20.5, 19.8; HRMS (ESI) calcd for  $\text{C}_{29}\text{H}_{28}\text{F}_2\text{N}_3\text{O}_2\text{RuS}^+ [\text{M} - \text{Cl}]^+ m/z$  622.0915, found  $m/z$  622.0918. Anal. Calcd for  $\text{C}_{29}\text{H}_{28}\text{ClF}_2\text{N}_3\text{O}_2\text{RuS}$ , C, 53.01; H, 4.29; N, 6.39. Found: C, 52.22; H, 4.59; N, 5.70.

**Complex 13.** To a solution of **3** (71 mg, 0.20 mmol) in 5 mL of MeOH were added  $\text{Et}_3\text{N}$  (55  $\mu\text{L}$ , 0.40 mmol) and  $[\text{Ru}(\text{bz})\text{Cl}_2]_2$  (50 mg, 0.10 mmol). After the mixture was stirred for 2 h, the precipitate was filtered and washed with MeOH and  $\text{Et}_2\text{O}$  to afford **13** (94 mg, 0.13 mmol, 83%): brown powder;  $R_f$  = 0.42 ( $\text{CH}_2\text{Cl}_2/\text{MeOH}$ : 95/5); mp >270 °C; IR 3070, 1596, 1472, 1299, 1155, 1135, 1084, 939, 908, 848, 821, 767, 695  $\text{cm}^{-1}$ ;  $^1\text{H}$  NMR (400 MHz,  $\text{CDCl}_3$ )  $\delta$  8.09 (d,  $J$  = 8.2 Hz, 2H), 7.88–7.85 (m, 3H), 7.66 (t,  $J$  = 7.6 Hz, 2H), 7.54 (m, 1H), 7.41 (d,  $J$  = 8.7 Hz, 1H), 7.17 (d,  $J$  = 7.8 Hz, 2H), 7.07 (t,  $J$  = 7.8 Hz, 1H), 6.63 (t,  $J$  = 7.8 Hz, 1H), 5.48 (s, 6H), 2.32 (s, 3H);  $^{13}\text{C}\{^1\text{H}\}$  NMR (100 MHz,  $\text{CDCl}_3$ )  $\delta$  155.7, 152.0, 148.7, 142.3, 137.7, 133.5, 129.3, 129.0, 128.9, 122.4, 119.6, 119.2, 118.7, 87.2, 21.6; HRMS (ESI) calcd for  $\text{C}_{25}\text{H}_{22}\text{N}_3\text{O}_2\text{RuS}^+ [\text{M} - \text{Cl}]^+ m/z$  530.0477, found  $m/z$  530.0476. Anal. Calcd for  $\text{C}_{25}\text{H}_{22}\text{ClN}_3\text{O}_2\text{RuS}$ , C, 53.14; H, 3.92; N, 6.27. Found: C, 52.59; H, 4.11; N, 7.37.

**Complex 14.** To a solution of **3** (32 mg, 0.09 mmol) in 3 mL of MeOH were added  $\text{Et}_3\text{N}$  (25  $\mu\text{L}$ , 0.18 mmol) and  $[\text{Ru}(\text{hmbz})\text{Cl}_2]_2$  (30 mg, 0.045 mmol). After the mixture was stirred for 15 h, the precipitate was filtered and washed with MeOH and  $\text{Et}_2\text{O}$  to afford **14** (44 mg, 0.068 mmol, 75%): black powder;  $R_f$  = 0.46 ( $\text{CH}_2\text{Cl}_2/\text{MeOH}$  95/5); mp 264 °C; IR 3736, 3051, 1593, 1470, 1301, 1137, 1085, 934, 850, 767, 679  $\text{cm}^{-1}$ ;  $^1\text{H}$  NMR (400 MHz,  $\text{CDCl}_3$ )  $\delta$  8.56 (d,  $J$  = 7.8 Hz, 2H), 7.96 (d,  $J$  = 8.7 Hz, 2H), 7.91 (d,  $J$  = 8.2 Hz, 1H), 7.72 (d,  $J$  = 8.7 Hz, 1H), 7.68–7.64 (m, 2H), 7.46 (t,  $J$  = 7.6 Hz, 1H), 7.08–7.02 (m, 3H), 6.61 (m, 1H), 2.24 (s, 3H), 1.83 (s, 18H);  $^{13}\text{C}\{^1\text{H}\}$  NMR (100 MHz,  $\text{CDCl}_3$ )  $\delta$  152.6, 151.5, 150.7, 141.5, 139.0, 131.9, 130.4, 129.6, 129.2, 128.9, 124.8, 120.6, 118.9, 117.7, 96.2, 21.5, 16.1; HRMS (ESI) calcd for  $\text{C}_{31}\text{H}_{34}\text{N}_3\text{O}_2\text{RuS}^+ [\text{M} - \text{Cl}]^+ m/z$  614.1417, found  $m/z$  614.1414. Anal. Calcd for  $\text{C}_{31}\text{H}_{34}\text{ClN}_3\text{O}_2\text{RuS}$ : C, 57.35; H, 5.28; N, 6.47. Found: C, 57.12; H, 5.36; N, 6.46.

**Computational Details.** All density functional theory (DFT) calculations were performed with the Gaussian09 package at the B3LYP level.<sup>65</sup> LanL2DZ and 6-31G\*\* (d,p) basis sets were used for Ru and all other atoms, respectively. The effect of solvent (acetonitrile) was taken into account by continuum CPCM single-point calculations on gas-phase optimized geometries. The absence of imaginary frequencies was checked on all calculated structures to confirm they are true minima.

## ■ ASSOCIATED CONTENT

### § Supporting Information

The Supporting Information is available free of charge on the ACS Publications website at DOI: 10.1021/acs.organo-met.5b00871.

NMR spectra, additional UV–vis absorption spectra, procedures for the determination of half-lives and *Z/E* ratios in the PSS, and details concerning X-ray structure determination (PDF)

All computed molecule Cartesian coordinates (XYZ)

Crystallographic data for **4**, **7**, **9**, and **14** (CIF)

## ■ AUTHOR INFORMATION

### Corresponding Authors

\*E-mail for N.B.: nicolas.bogliotti@ppsm.ens-cachan.fr.

\*E-mail for J.X.: joanne.xie@ens-cachan.fr.

### Notes

The authors declare no competing financial interest.

## ■ ACKNOWLEDGMENTS

We thank Dr. Gilles Clavier for helpful discussions concerning DFT calculations.

## ■ REFERENCES

- (1) Hu, Y.; Tabor, R. F.; Wilkinson, B. L. *Org. Biomol. Chem.* **2015**, *13*, 2216–2225.
- (2) Velema, W. A.; Szymanski, W.; Feringa, B. L. *J. Am. Chem. Soc.* **2014**, *136*, 2178–2191.
- (3) Li, J.; Wang, X.; Liang, X. *Chem. - Asian J.* **2014**, *9*, 3344–3358.
- (4) Kundu, P. K.; Klajn, R. *ACS Nano* **2014**, *8*, 11913–11916.
- (5) García-Iriepa, C.; Marazzi, M.; Frutos, L. M.; Sampedro, D. *RSC Adv.* **2013**, *3*, 6241–6266.
- (6) Wegner, H. A. *Angew. Chem., Int. Ed.* **2012**, *51*, 4787–4788.
- (7) Bandara, H. M. D.; Burdette, S. C. *Chem. Soc. Rev.* **2012**, *41*, 1809–1825.
- (8) Merino, E. *Chem. Soc. Rev.* **2011**, *40*, 3835–3853.
- (9) Beharry, A. A.; Woolley, G. A. *Chem. Soc. Rev.* **2011**, *40*, 4422–4437.
- (10) Hamon, F.; Djedaini-Pilard, F.; Barbot, F.; Len, C. *Tetrahedron* **2009**, *65*, 10105–10123.
- (11) Samanta, S.; Ghosh, P.; Goswami, S. *Dalton Trans.* **2012**, *41*, 2213–2226.
- (12) Pattanayak, P.; Parua, S. P.; Patra, D.; Lai, C.-K.; Brandão, P.; Felix, V.; Chattopadhyay, S. *Inorg. Chim. Acta* **2015**, *429*, 122–131.
- (13) Ding, F.; Sun, Y.; Verpoort, F. *Eur. J. Inorg. Chem.* **2010**, *2010*, 1536–1543.
- (14) Kannan, S.; Ramesh, R.; Liu, Y. J. *Organomet. Chem.* **2007**, *692*, 3380–3391.
- (15) Venkatachalam, G.; Ramesh, R. *Tetrahedron Lett.* **2005**, *46*, 5215–5218.
- (16) Rath, R. K.; Nethaji, M.; Chakravarty, A. R. *J. Organomet. Chem.* **2001**, *633*, 79–84.
- (17) Romero-Canelón, I.; Salassa, L.; Sadler, P. J. *J. Med. Chem.* **2013**, *56*, 1291–1300.
- (18) Dougan, S. J.; Habtemariam, A.; McHale, S. E.; Parsons, S.; Sadler, P. J. *Proc. Natl. Acad. Sci. U. S. A.* **2008**, *105*, 11628–11633.

- (19) Velders, A. H.; Kooijman, H.; Spek, A. L.; Haasnoot, J. G.; de Vos, D.; Reedijk, J. *Inorg. Chem.* **2000**, *39*, 2966–2967.
- (20) Dougan, S. J.; Melchart, M.; Habtemariam, A.; Parsons, S.; Sadler, P. J. *Inorg. Chem.* **2006**, *45*, 10882–10894.
- (21) Dinda, J.; Senapoti, S.; Mondal, T.; Jana, A. D.; Chiang, M. Y.; Lu, T.-H.; Sinha, C. *Polyhedron* **2006**, *25*, 1125–1132.
- (22) Govindaswamy, P.; Sinha, C.; Kollipara, M. R. *J. Organomet. Chem.* **2005**, *690*, 3465–3473.
- (23) Velders, A. H.; van der Schilden, K.; Hotze, A. C.; Reedijk, J.; Kooijman, H.; Spek, A. L. *Dalton Trans.* **2004**, 448–455.
- (24) Das, C.; Saha, A.; Hung, C.-H.; Lee, G.-H.; Peng, S.-M.; Goswami, S. *Inorg. Chem.* **2003**, *42*, 198–204.
- (25) Das, C.; Ghosh, A. K.; Hung, C.-H.; Lee, G.-H.; Peng, S.-M.; Goswami, S. *Inorg. Chem.* **2002**, *41*, 7125–7135.
- (26) Flower, K. R.; Pritchard, R. G. *J. Organomet. Chem.* **2001**, *620*, 60–68.
- (27) Rath, R. K.; Valavi, S. G.; Geetha, K.; Chakravarty, A. R. *J. Organomet. Chem.* **2000**, *596*, 232–236.
- (28) Mondal, B.; Walawalkar, M. G.; Kumar Lahiri, G. J. *Chem. Soc., Dalton Trans.* **2000**, 4209–4217.
- (29) Hotze, A. C. G.; Velders, A. H.; Ugozzoli, F.; Biagini-Cingi, M.; Manotti-Lanfredi, A. M.; Haasnoot, J. G.; Reedijk, J. *Inorg. Chem.* **2000**, *39*, 3838–3844.
- (30) Santra, P. K.; Misra, T. K.; Das, D.; Sinha, C.; Slawin, A. M.; Woollins, J. D. *Polyhedron* **1999**, *18*, 2869–2878.
- (31) Pattanayak, P.; Patra, D.; Pratihari, J. L.; Burrows, A.; Mahon, M. F.; Chattopadhyay, S. *Inorg. Chim. Acta* **2010**, *363*, 2865–2873.
- (32) Pratihari, J. L.; Bhaduri, S.; Pattanayak, P.; Patra, D.; Chattopadhyay, S. *J. Organomet. Chem.* **2009**, *694*, 3401–3408.
- (33) Samanta, S.; Singh, P.; Fiedler, J.; Zális, S.; Kaim, W.; Goswami, S. *Inorg. Chem.* **2008**, *47*, 1625–1633.
- (34) Kitaura, R.; Miyaki, Y.; Onishi, T.; Kurosawa, H. *Inorg. Chim. Acta* **2002**, *334*, 142–148.
- (35) Miyaki, Y.; Onishi, T.; Kurosawa, H. *Chem. Lett.* **2000**, *29*, 1334–1335.
- (36) Corrigan, J. F.; Doherty, S.; Taylor, N. J.; Carty, A. J. *J. Chem. Soc., Chem. Commun.* **1991**, 1640–1641.
- (37) Kume, S.; Nishihara, H. *Dalton Trans.* **2008**, 3260–3271.
- (38) Amar, A.; Savel, P.; Akdas-Kilig, H.; Katan, C.; Meghezzi, H.; Boucekkine, A.; Malval, J.-P.; Fillaut, J.-L. *Chem. - Eur. J.* **2015**, *21*, 8262–8270.
- (39) Göstl, R.; Senf, A.; Hecht, S. *Chem. Soc. Rev.* **2014**, *43*, 1982–1996.
- (40) Lee, H.-M.; Larson, D. R.; Lawrence, D. S. *ACS Chem. Biol.* **2009**, *4*, 409–427.
- (41) Lüning, U. *Angew. Chem., Int. Ed.* **2012**, *51*, 8163–8165.
- (42) Akita, M. *Organometallics* **2011**, *30*, 43–51.
- (43) Stoll, R. S.; Hecht, S. *Angew. Chem., Int. Ed.* **2010**, *49*, 5054–5075.
- (44) Samachetty, H. D.; Branda, N. R. *Pure Appl. Chem.* **2006**, *78*, 2351–2359.
- (45) Szymański, W.; Beierle, J. M.; Kistemaker, H. A. V.; Velema, W. A.; Feringa, B. L. *Chem. Rev.* **2013**, *113*, 6114–6178.
- (46) Brieke, C.; Rohrbach, F.; Gottschalk, A.; Mayer, G.; Heckel, A. *Angew. Chem., Int. Ed.* **2012**, *51*, 8446–8476.
- (47) Mayer, G.; Heckel, A. *Angew. Chem., Int. Ed.* **2006**, *45*, 4900–4921.
- (48) Wang, H.; Yu, Y.; Hong, X.; Tan, Q.; Xu, B. *J. Org. Chem.* **2014**, *79*, 3279–3288.
- (49) Rivillo, D.; Gulyás, H.; Benet-Buchholz, J.; Escudero-Adán, E. C.; Freixa, Z.; van Leeuwen, P. W. N. M. *Angew. Chem., Int. Ed.* **2007**, *46*, 7247–7250.
- (50) Brown, E. V.; Granneman, G. R. *J. Am. Chem. Soc.* **1975**, *97*, 621–627.
- (51) Knie, C.; Utecht, M.; Zhao, F.; Kulla, H.; Kovalenko, S.; Brouwer, A. M.; Saalfrank, P.; Hecht, S.; Bléger, D. *Chem. - Eur. J.* **2014**, *20*, 16492–16501.
- (52) Bléger, D.; Schwarz, J.; Brouwer, A. M.; Hecht, S. *J. Am. Chem. Soc.* **2012**, *134*, 20597–20600.
- (53) Bellotto, S.; Reuter, R.; Heinis, C.; Wegner, H. A. *J. Org. Chem.* **2011**, *76*, 9826–9834.
- (54) Martínez-Alonso, M.; Busto, N.; Jalón, F. A.; Manzano, B. R.; Leal, J. M.; Rodríguez, A. M.; García, B.; Espino, G. *Inorg. Chem.* **2014**, *53*, 11274–11288.
- (55) Bugarcic, T.; Habtemariam, A.; Deeth, R. J.; Fabbiani, F. P. A.; Parsons, S.; Sadler, P. J. *Inorg. Chem.* **2009**, *48*, 9444–9453.
- (56) Giannini, F.; Geiser, L.; Paul, L. E. H.; Roder, T.; Therrien, B.; Süß-Fink, G.; Furrer, J. *J. Organomet. Chem.* **2015**, *783*, 40–45.
- (57) Štěpnička, P.; Ludvík, J.; Canivet, J.; Süß-Fink, G. *Inorg. Chim. Acta* **2006**, *359*, 2369–2374.
- (58) Canivet, J.; Labat, G.; Stoeckli-Evans, H.; Süß-Fink, G. *Eur. J. Inorg. Chem.* **2005**, *2005*, 4493–4500.
- (59) Canivet, J.; Karmazin-Brelot, L.; Süß-Fink, G. *J. Organomet. Chem.* **2005**, *690*, 3202–3211.
- (60) Reichardt, C. In *Solvents and Solvent Effects in Organic Chemistry*; Wiley-VCH: Weinheim, Germany, 2003; pp 389–469.
- (61) Reichardt, C. *Pure Appl. Chem.* **1982**, *54*, 1867–1884.
- (62) Reichardt, C. In *Solvents and Solvent Effects in Organic Chemistry*; Wiley-VCH: Weinheim, Germany, 2003; pp 147–328.
- (63) Hansch, C.; Leo, A.; Taft, R. W. *Chem. Rev.* **1991**, *91*, 165–195.
- (64) Stang, P. J.; Anderson, A. G. *J. Org. Chem.* **1976**, *41*, 781–785.
- (65) Frisch, M. J.; Trucks, G. W.; Schlegel, H. B.; Scuseria, G. E.; Robb, M. A.; Cheeseman, J. R.; Scalmani, G.; Barone, V.; Mennucci, B.; Petersson, G. A.; Nakatsuji, H.; Caricato, M.; Li, X.; Hratchian, H. P.; Izmaylov, A. F.; Bloino, J.; Zheng, G.; Sonnenberg, J. L.; Hada, M.; Ehara, M.; Toyota, K.; Fukuda, R.; Hasegawa, J.; Ishida, M.; Nakajima, T.; Honda, Y.; Kitao, O.; Nakai, H.; Vreven, T.; Montgomery, J. A., Jr.; Peralta, J. E.; Ogliaro, F.; Bearpark, M. J.; Heyd, J.; Brothers, E. N.; Kudin, K. N.; Staroverov, V. N.; Kobayashi, R.; Normand, J.; Raghavachari, K.; Rendell, A. P.; Burant, J. C.; Iyengar, S. S.; Tomasi, J.; Cossi, M.; Rega, N.; Millam, N. J.; Klene, M.; Knox, J. E.; Cross, J. B.; Bakken, V.; Adamo, C.; Jaramillo, J.; Gomperts, R.; Stratmann, R. E.; Yazyev, O.; Austin, A. J.; Cammi, R.; Pomelli, C.; Ochterski, J. W.; Martin, R. L.; Morokuma, K.; Zakrzewski, V. G.; Voth, G. A.; Salvador, P.; Dannenberg, J. J.; Dapprich, S.; Daniels, A. D.; Farkas, Ö.; Foresman, J. B.; Ortiz, J. V.; Cioslowski, J.; Fox, D. J. *Gaussian 09*; Gaussian, Inc., Wallingford, CT, USA, 2009.
- (66) Jia, X.; Han, J. *J. Org. Chem.* **2014**, *79*, 4180–4185.